Stack velocity estimation trough a VFSA/Gauss-Newton hibrid algorithm

Danian S. Oliveira* Paulo E. M. Cunha* Milton J. Porsani** , *Petrobrás **CPGG/UFBA and INCT-GP/CNPQ

This paper was prepared for presentation at the 13th International Congress of the Brazilian Geophysical Society, held in Rio de Janeiro, Brazil, August 26-29, 2013.

Abstract

We developed a strategy for automatic construction of the stacking velocity field. This strategy is divided into two steps. The first step performs the automatic pick in Semblance panels through the Genetic Algorithm optimization method. In conjunction with restrictions and penalties set from *a priori* information it was obtained as a result a nonlinear fit of time interval velocities, that when converted at root mean square (RMS) velocity, better maximizes the sum of the common midpoint (CMP) group, corrected with normal moveout (NMO). This interval velocity field becomes the initial model of the inversion's second phase that uses a Very Fast Simulated Anealling and Gauss-Newton hybrid algorithm. From an initial velocity model and a Zero-Offset seismic section *a priori*, we try to find what the best field that generated this same section. Currently, there are extrapolation techniques that allow us to generate the zero-offset traces without the requirement of the velocity field. These traces may compose the zero-offset seismic section *a priori* in this second stage of this inversion strategy.

Introduction

Currently the good imaging of depp reflectors deep, especially in Brazilian basins, below the salt layer, has proved a major challenge. Obtaining a seismic velocity field corresponding to the subsurface geology and resulting in a focused seismic image is the main target of seismic processing.

In the last decade, the reflection tomography has established itself as one of the main methods of construction of velocity model for migration of seismic data. In a complex geological environment reflection tomography showed good results in the determination of seismic velocity field Clapp et al. (2004). Full waveforma inversion (FWI) returns due to recent advances in computing that enabled the use of this technique for the inversion of velocity models 2D and 3D Virieux Operto (2009) and also because of the great success in geologically complex scenarios. Despite the stacking velocity analysis be, among these, the less accurate method for generating velocity field it is still used on a large scale by oil and seismic processing companies beacause it is less expensive and can provide a good initial field for methods of tomography and FWI.

Inversion Strategy

The inversion of stacking velocity field is the subject of this study. This nonlinear problem was divided into two stages to better constrain the inversion. The first step was based on Lumley (1997) and uses Genetic Algorithm to do the automatic adjustment of the panels Semblance Oliveira et al. (2012).

The velocity field obtained in this step enters as the initial model for the second inversion strategy which utilizes a Very Fast Simulated Annealing and Gauss-Newton hybrid algorithm, where one tries to find the velocity model which produces a stacked seismic section *a priori*. To validate and assist in the description of the first strategy we used a synthetic seismic data (Figure 1). The CMP groups were generated by the convolution of a pulse of 20 Hz Ricker with Dirac deltas positioned on the transit time calculated analytically by the equation of NMO (equation 2).

To assess the second step we used a stacked section*a priori* of Jequitinhonha's Basin real seismic data. It was generated by NMO correction of the CMP's gathers and stacked with the velocity that will be considered as benchmark. The hybrid algorithm tries to find out what is the velocity that generated the stacked section*a priori*. If the algorithm is correct the inverted velocity model will approach the benchmark velocity field.

Direct Modeling and Otmization Methods

In a classic problem of inversion **d = Gm**, the matrix **G** relates the model **m** to the observed **d**. In this work the matrix **G** can be understood as the process of NMO correction and stacking working in CMP's gathers and the model is the interval stacking velocity in time . The main problem to be solved in the first stage of inversion revolves around Semblance panels. The second phase inversion uses only the correction of normal move out and stacking Castle (1994); de Bazelaire (1988)

$$\Delta\mathbf{t}_{nmo} = \mathbf{t}_{nmo} - \mathbf{t}_0, \tag{1}$$

onde

$$\mathbf{t}_{nmo} = \mathbf{t}_0\sqrt{1+\left(\frac{\Delta\mathbf{x}}{\mathbf{v}\mathbf{t}_0}\right)}, \tag{2}$$

The amplitudes values are normalized by the Semblance equation Taner Koehler (1969).

$$NE = \frac{1}{m}\frac{\sum_{n=1}\sum_{i=1}\mathbf{f}_{i,n}}{\sqrt{\sum_{n=1}\sum_{i=1}\mathbf{f}_{i,n}^2}} \tag{3}$$

The global search optimization method Genetic Algorithm (GA), used for automatic adjustment of Semblance, generates an initial population of interval velocity models and converts the values of the parameter space in binary where the number of bits of the binary has a relation (equation 4) to the number of model parameters.

$$npar = nbits^2 - 1 \tag{4}$$

Parameter	Value	Position	Binary value
V	1500m/s	1	00
	2000m/s	2	01
$\mathrm{N}_v = 3$	2500m/s	3	11

Table 1: Example binary encoding of the velocity parameter.

The main feature of Genetic Algorithm is application of three procedures on models initial population, which aim to generate the models descendants, better than the initial population. This does there is a rapid convergence to the solution .

The tree processes are selection, crossover and mutation. The evaluation of models of the initial population as well as descendants models is called fitness. This value controls whether a model is accepted or rejected. The Semblance adjustment with AG was performed in two stages. The first was denominated parametric inversion (Figure 2) which fits a RMS velocity function that maximizes the integration of Semblance, following the equation

$$v = v0 + \alpha t^{\beta} \tag{5}$$

The values to be inverted are v0, which is the initial speed or the water surface, the velocity gradient (α) and β, which may be understood as the curvature of the velocity function. The RMS velocity function built in this step (Figure 3) becomes the guide used to define the space of modelsof the second stage of inversion that performs nonlinear fitting of Semblance (Figure 4). From the guide function are generated several random time interval velocities models. It was made the fitness measure of these modelsand then they suffer GA processes in n iterations until some stopping criterion is satisfied. The inverted velocity model (Figure 4) can be compared with the real model (Figure 5). The whole ideia is use the model set by AG as a initial model for the Very Fast Simulated Anealling/Gauss newton inversion. The VFSA generate a perturbation in the initial model $\mathbf{\Delta m}^k$

$$\mathbf{m}^{k+1} = \mathbf{m}^k + \mathbf{y}(\mathbf{m}^{max} - \mathbf{m}^{min}), \tag{6}$$

where **y** $\in [-1,1]$ e $\mathbf{m}^{min} \leq \mathbf{m}^{k+1} \leq \mathbf{m}^{max}$ Varela (1996).

The perturbation, which depends on temperature T^k, is a Cauchy distribution type

$$g_T = \prod_{i=1}^{NM} \frac{1}{2(|y_i| + T_i)ln\left(1 + \frac{1}{T_i}\right)}. \tag{7}$$

If we sort a number from a uniform distribution $U[0,1]$ the parameter y_i may be mapped in the distribution above using the following equation

$$y_i = sgn\left(u_i - \frac{1}{2}\right)T_i\left[\left(1 + \frac{1}{T_i}\right)^{|2u_i-1|} - 1\right]. \tag{8}$$

The exponential cooling scheme of VFSA is given by the equation 9 where T_i^0 is the temperature of the parameter i of the space model and c_i is a parameter defined by user that adjusts the algorithm for specific problems.

$$T_i^k = T_i^0 exp(-c_i k^{1/NM}), \tag{9}$$

Results

Were performed the automatic Semblanceon adjustment in real seismic data of Jequitinhonha's Basin (Figura 6). One can assess the non linear fit fof the first inversion step by Figure 7. The black curves represent the RMS velocity and the red ones, the time interval velocities. The convergence curve (Figure 8) shows the normalized fitness of the populations in each generation. The red curve represents the best fitness, while the the blue teh worst. The final result is a 2D time interval velocity field that best fits the Semblance (Figure 10). This velocity field obtained by nonlinear fit of the Semblance becames the initial model for the next inversion step performed by a hybrid algorithm VFSA/Gauss-Newton. From the stacked section stacked (Figure 11) with the benchmark velocity (Figure 12) through the this inversion strategy, we obtained the time interval velocity field (Figure 13) which can be compared with the benchmark velocity field (Figura 11). The errors of the stacked seismic section with inverted fields in both steps within the stacked section with the benchmark velocity are described in Table 2. The convergence curve in Figure 9 shows the improvement of the model between reheating steps due to intervention of the Gauss-Newton optmization method.

Inversion step	2D *RMS* normalized error
Scan fit with GA	0.79990351
VFSA Gauss-Newton Vel. refine	0.46243998

Table 2: 2D *RMS* error of the stacked seismic section with the velocity obtained in the two inversion steps within the stacked section generated with the benchmark velocity.

Discussion and Conclusions

We tested several optimization methods and applied it in two independent and complementary methodologies to automatic generation of stacking velocities field thats has geological coherence when converted to interval velocity. Despite the second strategy depends on Zero-Offset section, it is possible to generate it without a velocity field (Landa (2007); Verschuur (2006)), which makes this inversion methodology interesting form the industrial point of view. .

References

Castle, R. J., 1994, A theory of normal moveout: Geophysics, **59**, 983–999.

Clapp, R. G., , et al., 2004, Incorporating geologic information into reflection tomography: Geophysics, **69**, no. 2.

de Bazelaire, E., 1988, Normal moveout revisited: Inhomogeneous media and curved interfaces: Geophysics, **53**, no. 2, 143–157.

Landa, E., 2007, Beyond conventional seismic imaging:, Education Tour Series EAGE Publications bv, The Netherlands.

Lumley, D. E., 1997, Monte carlo automatic velocity picks: SEP Report, **75**, 1–25.

Oliveira, D. S., Porsani, M. J., Cunha, P. E. M., 2012, Determinação do campo de velocidades de empilhamento utilizando o algorítmo genético: V Simpósio Brasileiro de Geofísica, Expanded Abstracts.

Taner, M. T., Koehler, F., 1969, Velocity spectra digital computer derivation and applications of velocity functions: Geophysics, **34**, 859–881.

Varela, C. L., 1996, Automatic background velocity estimation in 2d laterally varying media: Ph.D. thesis, The University of Texas at Austin Institute for Geophysics, Austin/Texas/USA.

Verschuur, D. J., 2006, Seismic multiple removal, past, present and future:, Education Tour Series EAGE Publications bv, The Netherlands.

Virieux, J., Operto, S., 2009, An overview of full-waveform inversion in exploration geophysics: Geophysics, **74**, no. 6.

Acknowledgments

We would like to thank PETROBRAS and CNPq/INCT-GP for suporting this research.

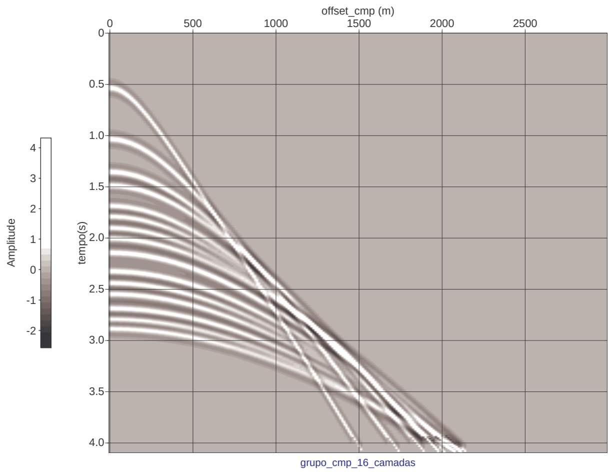

Figure 1: Synthetic CMP gather.

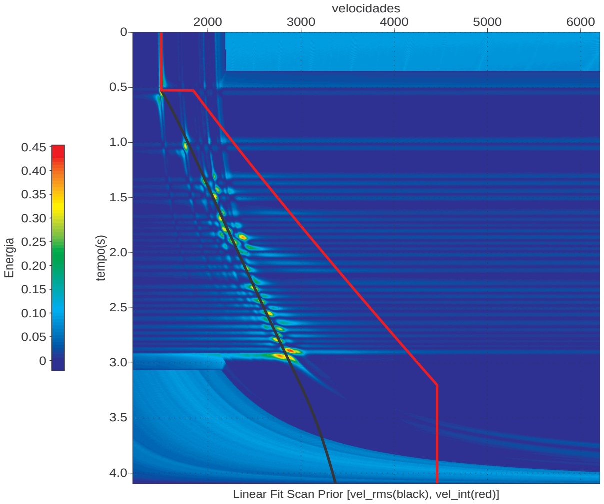

Figure 2: Parametric fit of the sinthetic model.

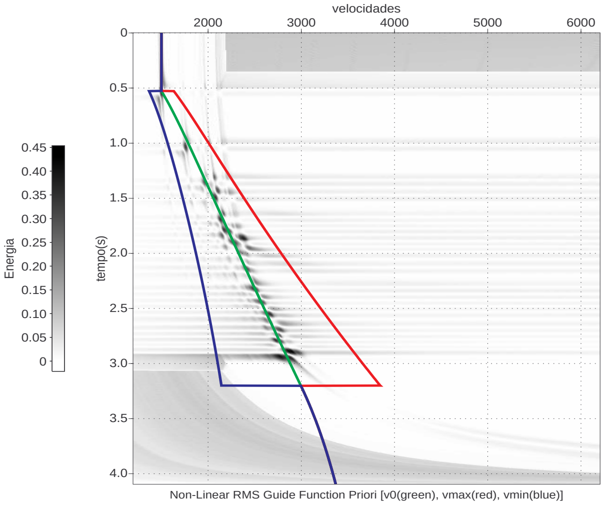

Figure 3: Model space generated from the guide function.

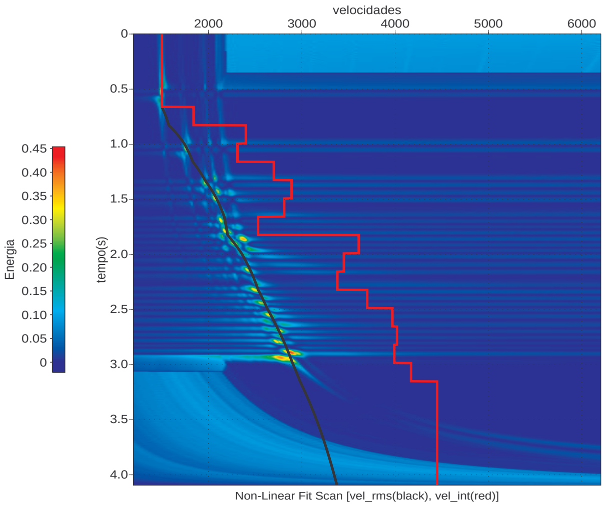

Figure 4: Non linear fit of the sinthetic model

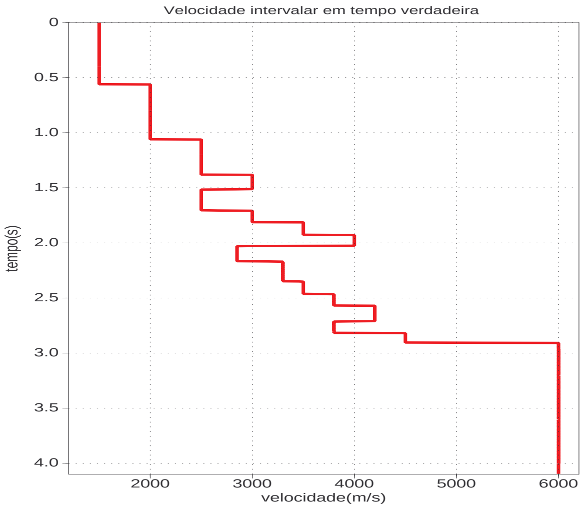

Figure 5: True sinthetic interval velocity function in time

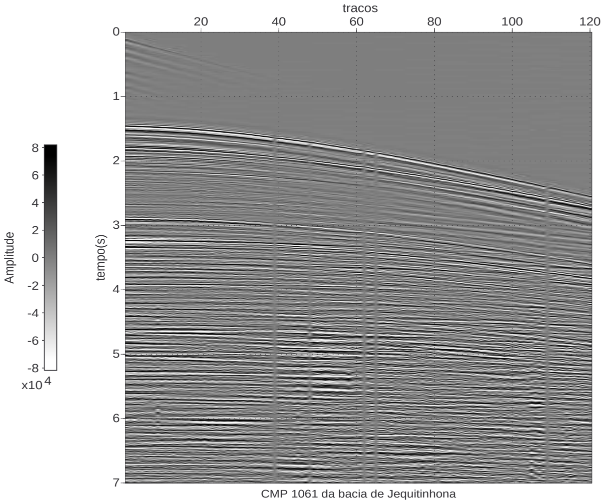

Figure 6: CMP gather of Jequitinhonha's Basin.

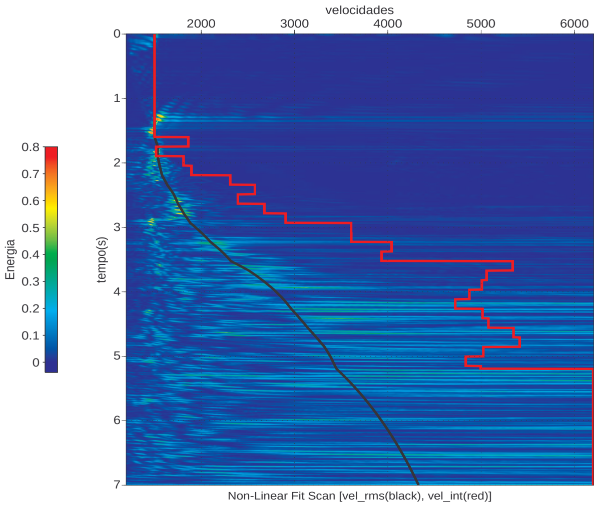

Figure 7: Non linear scan fit of one CMP in Jequitinhonha's Basin.

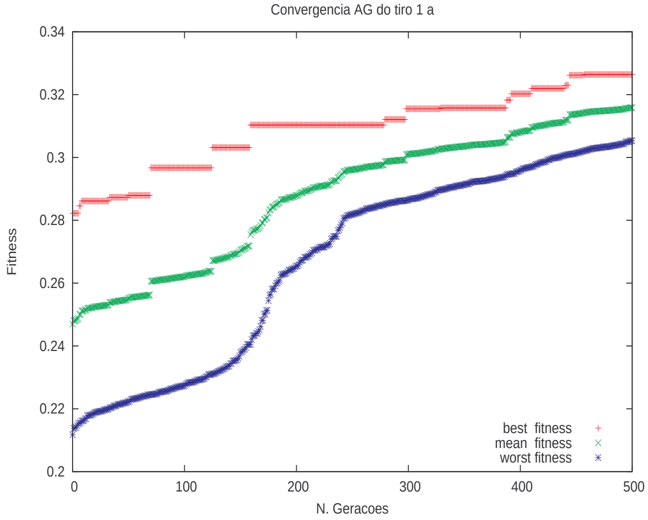

Figure 8: Convergence curve of one CMP in Jequitinhonha's Basin .

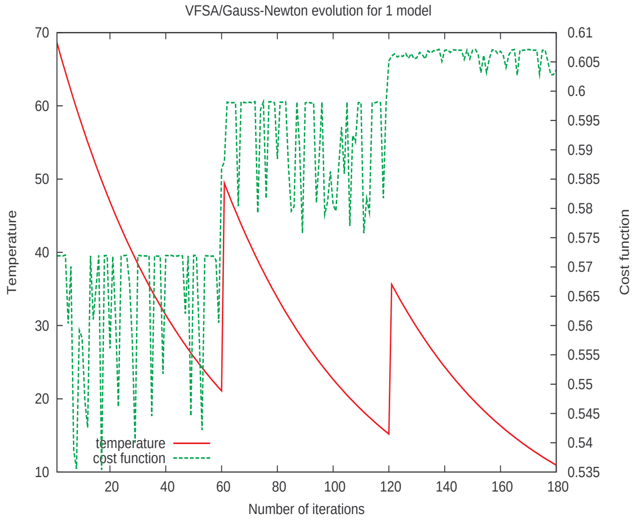

Figure 9: Convergence curve of VFSA/Gauss-Newton algorith with the temperature and the energy of the first model parameter.

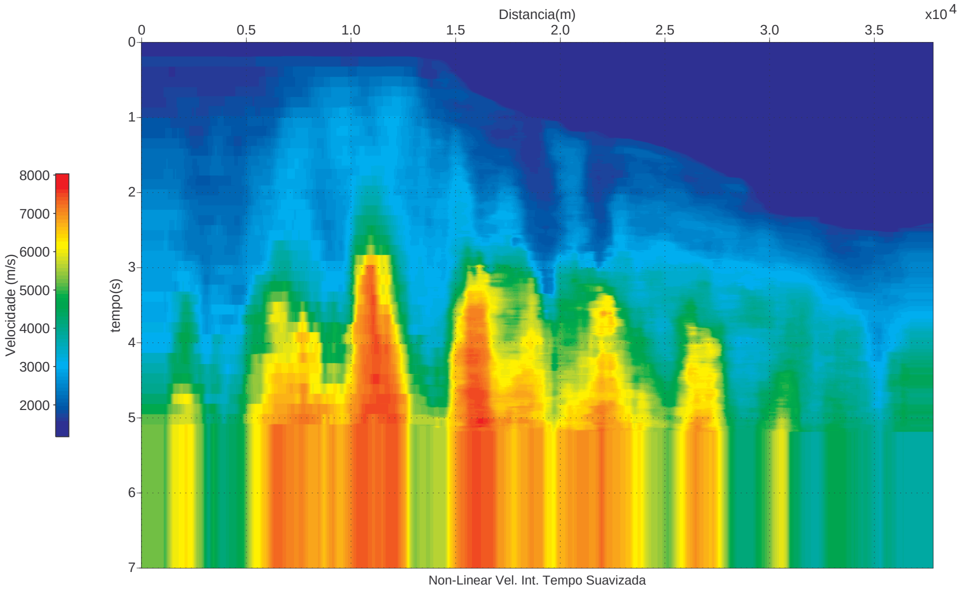

Figure 10: Interval velocity field in time inverted in the first inversion step and initial model for the second inversion step.

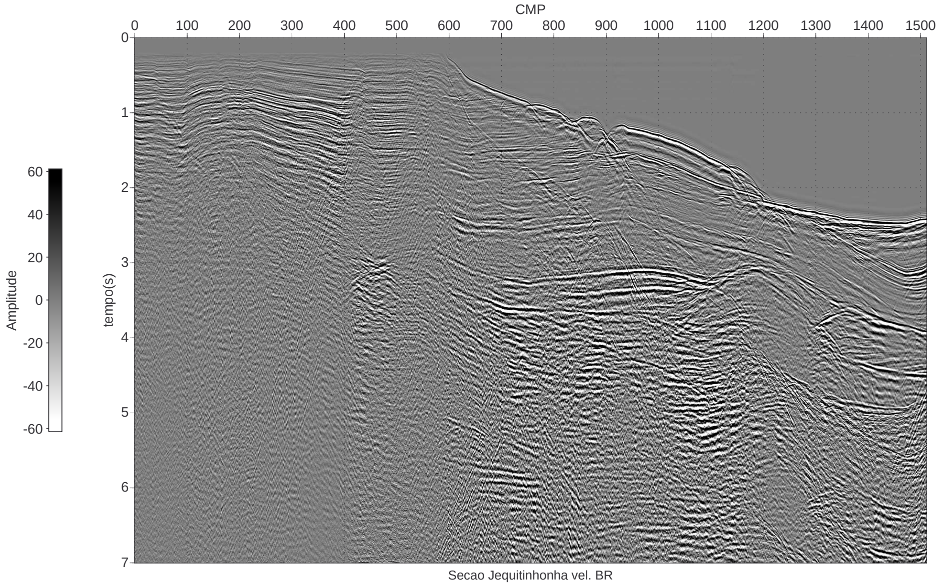

Figure 11: Stacked seismic section of Jequitinhonha's Basin with the benchmark velocity model.

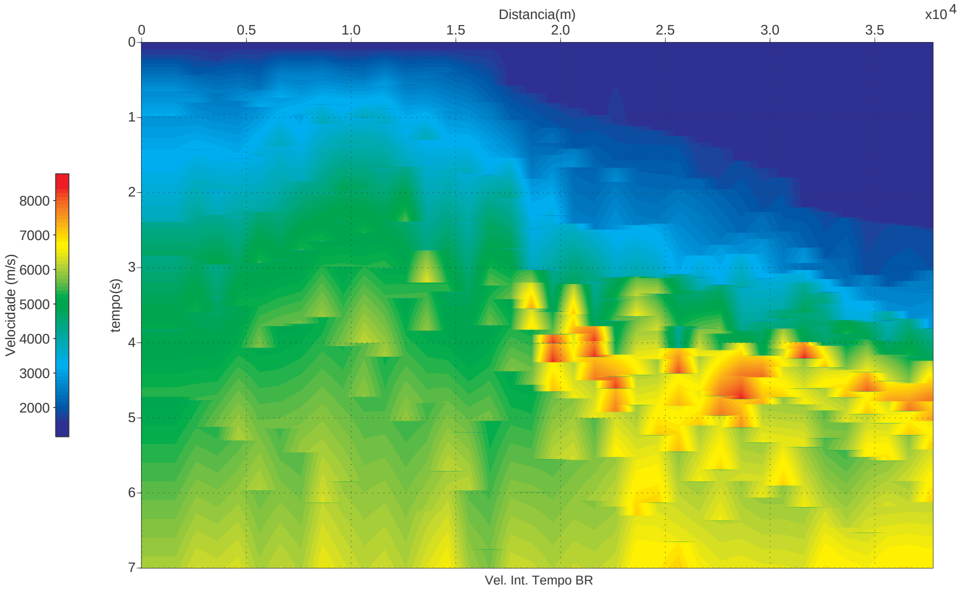

Figure 12: Benchmark interval velocity field in time of Jequitinhonha's Basin.

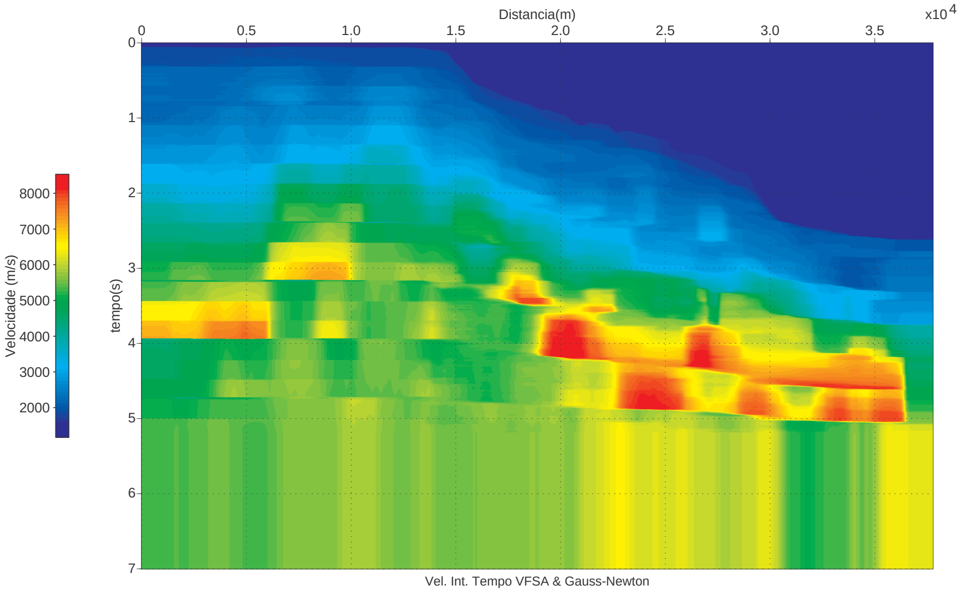

Figure 13: Interval velocity field in time of Jequitinhonha's Basin inverted in the second inversion step (VFSA/Gauss-Newton).